N91-20642

RESOLVED RATE AND TORQUE CONTROL SCHEMES FOR LARGE SCALE SPACE BASED KINEMATICALLY REDUNDANT MANIPULATORS

Robert W. Bailey
LinCom Corporation
1020 Bay Area Blvd, Suite 200
Houston, Tx 77058

Leslie J. Quiocho
Robotic Systems Evaluation Branch - ER4
Automation and Robotics Division
NASA/Lyndon B. Johnson Space Center
Houston, Tx 77058

ABSTRACT

Resolved rate control of kinematically redundant ground based manipulators is a challenging, but well understood problem. The structural, actuator, and control loop frequency characteristics of industrial grade robots generally allow operation with resolved rate control -- a rate command is achievable with good accuracy. However, space based manipulators are quite different, typically having less structural stiffness, more motor and joint friction, and lower control loop cycle frequencies. These undesirable characteristics present a considerable Point of Resolution (POR) control problem for space based, kinematically redundant manipulators for the following reason: a kinematically redundant manipulator requires an arbitrary constraint to solve for the joint rate commands. A space manipulator will assuredly not respond to joint rate commands as expected because of these undesirable characteristics. The question is, will low frequency rate feedback be adequate for POR control, and if not, what type of control scheme will be adequate? A space based manipulator simulation, including free end rigid body dynamics, motor dynamics, motor stiction/friction, gearbox backlash, joint stiction/friction, and Space Station RMS type configuration parameters, is utilized to evaluate the performance of a well documented resolved rate control law. Alternate schemes involving combined resolved rate and torque control are also evaluated.

INTRODUCTION

Space based manipulator design imposes a more stringent control problem than does ground based design. Space manipulators must be as light as possible to avoid excessive earth to orbit transportation costs. Space manipulators must also be able to survive the vacuum conditions on orbit. These design requirements produce manipulators with light-weight structures, large gear-ratios (relatively large backlash regions), high frequency low torque motors, excessive joint and motor friction, and low frequency control loop cycles (flight qualified computers which are slow compared to today's technology). To compound these physical contributions to the control problem, a kinematically redundant manipulator inherently allows an infinite number of arm configurations to achieve a given Point Of Resolution (POR) Cartesian position and orientation. This redundancy has its advantages and disadvantages. One such advantage is that infinite joint solutions allows a diverse range of control schemes. However, a disadvantage is that it can contribute to arm configuration drift through a given POR maneuver. In this paper, we will conceptually explain this problem and support the explanation with dynamic and kinematic simulation analysis of a Space Station RMS type manipulator. Variations of the classic motor rate feedback control system based on POR force and torque control will also be discussed as a possible solution to the problem.

PROBLEM CONCEPTUALIZATION

The majority of Space Station assembly analysis is currently being performed with kinematic manipulator simulations. Assuming that the actual space-based manipulator will respond exactly as the kinematically simulated manipulator, operational scenarios developed using the kinematic simulation will be adequate for space operations. This assumption could lead to dangerous consequences if kinematic control is not augmented with dynamic simulation. Several aspects of space manipulator operations will contribute to a drift (compared to kinematic simulation response) in the arm configuration through a given POR maneuver. Note that the problem of a drifting arm configuration from expected results is an entirely different problem from fundamental control of the manipulator POR.

Space based manipulator joint state responses have the following characteristics:

1) discontinuities - due to joint and motor stiction,
2) non-linearities - due to motor gearbox backlash (flexibility), and
3) variations - due to changing mass properties of the system.

In addition, actively controlled joint state responses have the following characteristics:

1) discontinuities - due to low frequency control loops,
2) non-linearities - due to joint state feedback, and
3) variations - due to constant control gains applied to changing system.

All of these characteristics contribute to a different joint response between actual dynamic manipulator systems and kinematically simulated manipulator systems. A standard resolved rate POR control scheme can effectively control the POR trajectory, but it can do little to control the joint trajectories. For a kinematically redundant manipulator, an infinite number of joint trajectories are possible for any given POR maneuver. Because of this, an actual space manipulator response (with a conventional resolved rate POR controller) is guaranteed to be different from a kinematic simulation response for the maneuver. Through a complex sequence of POR maneuvers (such as those proposed for Space Station assembly), the drift in the arm configuration between actual manipulator and simulated manipulator response will continue to grow through each successive maneuver potentially creating dangerous operational problems.

ANALYSIS OVERVIEW

To demonstrate the concepts and problems discussed above, two simulations runs are performed – one kinematic and one dynamic. A brief overview of the simulation math models is presented later. The kinematic simulation run consists of a POR maneuver, with acceleration and deceleration profiles, and an active position hold region. The dynamic simulation run consists of the exact same maneuver and position hold commands. The differences in the responses of the two simulations are discussed in detail to provide a better understanding of the control problems discussed above.

In addition to these runs, a second dynamic simulation is also performed incorporating POR force/torque control (instead of resolved rate control) during maneuver acceleration and deceleration regions. Results from this simulation are used to show advantages and disadvantages of stand-alone POR force/torque control.

Simulation Description

The kinematic simulation flow is depicted in Figure 1. The dynamic simulation flow is depicted in Figure 2. The manipulator guidance and control blocks of each simulation are *identical* to ensure proper comparison between the kinematic and dynamic simulations. With perfect sensing and perfect joint servos, the kinematic simulation is reduced to direct integration of the joint rate commands to produce joint positions; state integration and the control loop cycle times are both set to 80 milliseconds. The dynamic simulation, with perfect analog-to-digital conversion and perfect sensing, has a higher fidelity motor model including friction compensation logic for joint rate and torque commands, motor and joint friction, and joint gearbox backlash. As with the kinematic simulation, the manipulator guidance and control block for the dynamic simulation is also performed every 80 milliseconds. However, state integration is performed every 5 milliseconds with a fourth order modified midpoint integration scheme (3 step with 2 acceleration evaluations) [1].

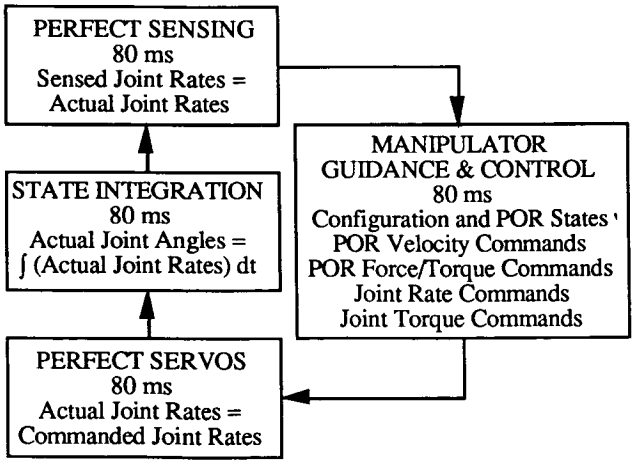

Figure 1 - Kinematic Simulation Flow

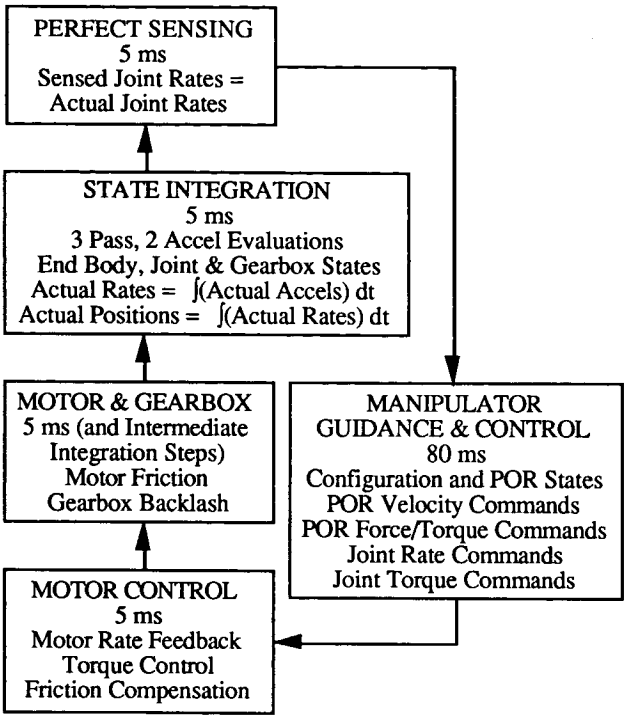

Figure 2 - Dynamic Simulation Flow

The manipulator guidance and control block is shown in Figure 3. There are two important aspects of this diagram, POR rate control and POR force/torque control Rate control will be discussed first and then force/torque control.

For POR rate control, pointing vectors from the current POR states to the desired POR states are unitized and scaled by the POR maneuver rates to produce the POR rotational and translational commands. These commands are then scaled, depending on the current maneuver region, to produce the final POR rate commands. There are four distinct maneuver regions: acceleration, maneuver, deceleration, and active position hold. For each of these regions, POR rotation and translation commands are completely decoupled, i.e., POR rotation could be in the acceleration region while POR translation is in the active position hold region.

During the acceleration region, the POR rate command vectors are scaled based on elapsed time from zero to the maneuver rates thus emulating a constant acceleration profile. During the maneuver region, the commanded POR rates remain unchanged. During the deceleration and active position hold regions, the commanded POR rates are scaled from the maneuver rates to zero based on the "distance-to-go" to the desired POR end states; this function produces a parabolic velocity profile during braking. Using the final POR rate commands, joint rate commands are then generated via the resolved rate control law proposed by Whitney with constant unity weighting [2,3]. With the joint rate commands in hand, a gain for the friction compensation logic located in the motor model is calculated to provide a smooth transition for the friction compensation commands as the joint rates change direction. The motor model also contains a rate feedback loop.

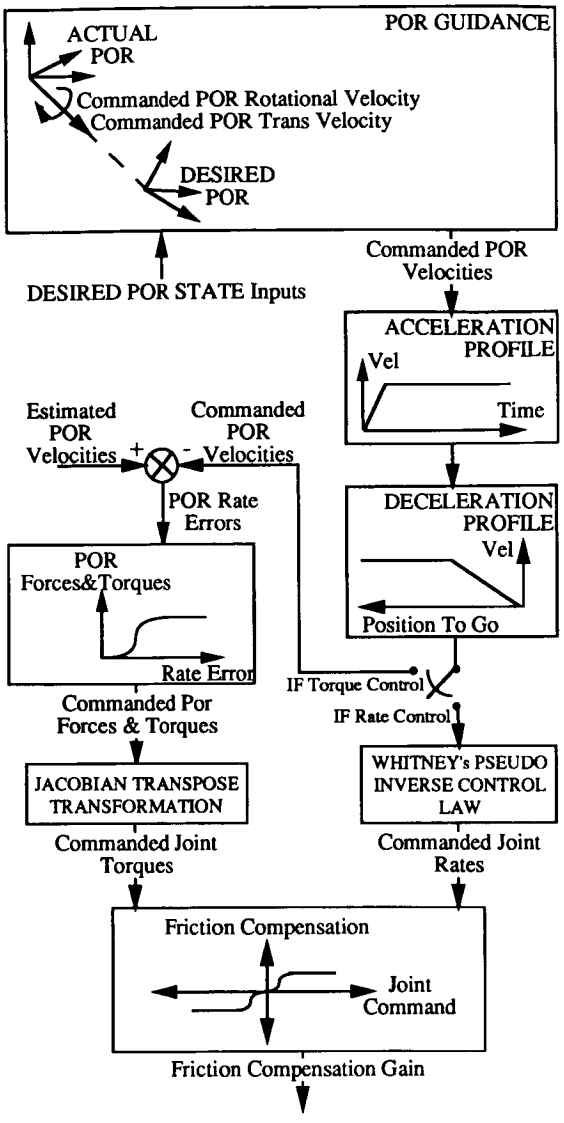

Figure 3 - Manipulator POR Guidance and Joint Rate/Torque Control

The POR force/torque control depends to a great extent on the existing POR rate control. The primary difference between the two control schemes is that during rate control, joint rate feeds back directly to the joint rate commands at a high frequency, but for force/torque control, the joint rate feedback is transformed to POR rate feedback and performed at a low frequency. Also, for the current analyses, the force/torque control is used only during the acceleration and deceleration maneuver regions. For these regions, the POR rates are fed back into the POR rate commands to produce POR rate error vectors. These vectors are unitized and then scaled from zero to the maximum maneuver forces and torques based upon the magnitude of the rate error vectors. These final commanded POR force and torque vectors are then transformed to joint torques via the transpose of the Jacobian matrix. Friction compensation gains again must be calculated to provide a smooth transition when the joint torque commands change directions.

The dynamic simulation motor model, presented in Figure 4, accepts both the joint rate and the joint torque commands. Torque commands are scaled directly to applied motor voltage (after gear reduction), while the rate commands go through gear reduction and are then differenced with the actual motor rates (rate feedback) before being scaled to applied motor voltages. Both sets of applied motor voltages are summed along with a friction compensation voltage that acts in the direction of the commanded joint rate (a simplistic description) to offset the effects of motor and joint friction. The resulting motor voltage is scaled to produce the applied motor torque. For this analysis, applied motor torque is calculated at 200 Hz (5 milliseconds).

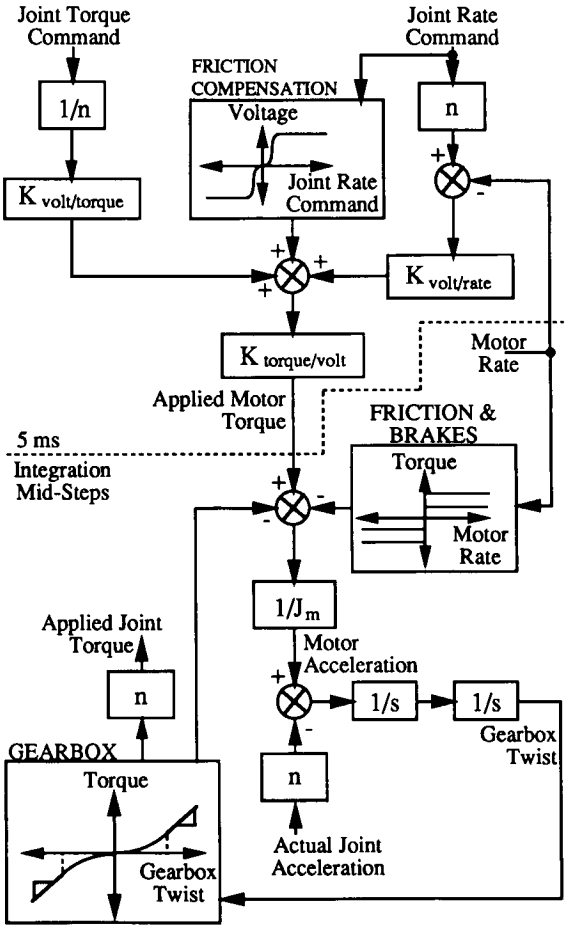

Figure 4 - Motor Rate/Torque Control and Gearbox Dynamics

Continuing with Figure 4, motor acceleration is determined by subtracting the torque due to motor friction and the gearbox torque from the applied motor torque, and dividing by the motor shaft inertia. This acceleration is differenced with the actual joint acceleration (after gear reduction) to produce the gearbox twist acceleration. The gearbox twist acceleration is then integrated twice to produce the gearbox twist angle used to determine the gearbox torque through a two stage gearbox backlash model. The first stage is non-linear to a breakout angle; the second stage is linear past the breakout angle. For the current analysis, gearbox twist state integration is performed over a 5 millisecond time step with the modified midpoint integration scheme; intermediate steps are synchronized with the joint state integration (from the manipulator dynamics).

Data Loads and Preparation

The manipulator system simulated consists of a Space Shuttle base vehicle (mass characteristics), a SPAS satellite payload (mass characteristics), and a Space Station RMS (mass and kinematic configuration). Data Loads for the simulations are taken primarily from published documents for the Space Shuttle, the Shuttle RMS, and the Space Station RMS. Mass Properties and attach point information for the Shuttle and the SPAS satellite payload are extracted from the PDRSS data book. Mass properties and kinematic configuration data for the SSRMS are extracted from a SPAR document. The motor, gearbox, and friction data for all 7 SSRMS joints is of the SRMS shoulder yaw joint, also from the PDRSS document. The torque to voltage and voltage to torque gains in the motor model also correspond to the SRMS shoulder yaw joint. Maneuver rates, tolerances, and breaking thresholds all correspond to specified data given for the SRMS manipulating the SPAS satellite. The maneuver selected for analysis is arbitrary with maneuver initial and final manipulator configurations depicted in Figures 5 and 6 respectively.

The motor model rate to voltage control gain was determined individually for all seven joints. First, brakes were applied on all joints. Next, brakes were relieved for a single joint and that joint was commanded to achieve a specified mid-range rotation rate. The rate to voltage gain was adjusted for the joint until the joint response yielded good acceleration and rate maintenance qualities. The initial configuration of the arm was identical for all control tests and significantly different from any of the configurations achieved during POR maneuver analysis.

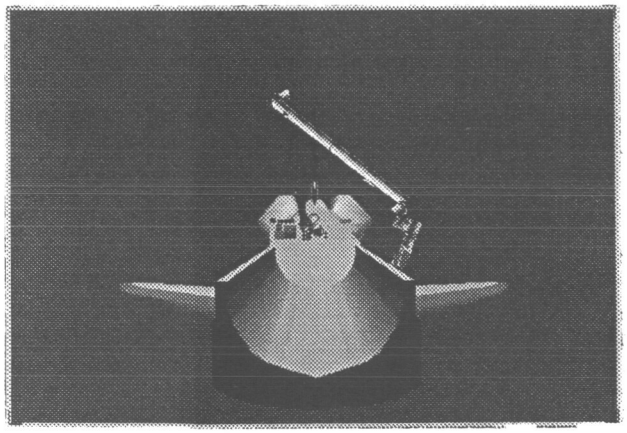

Figure 5 - POR Maneuver Initial Configuration

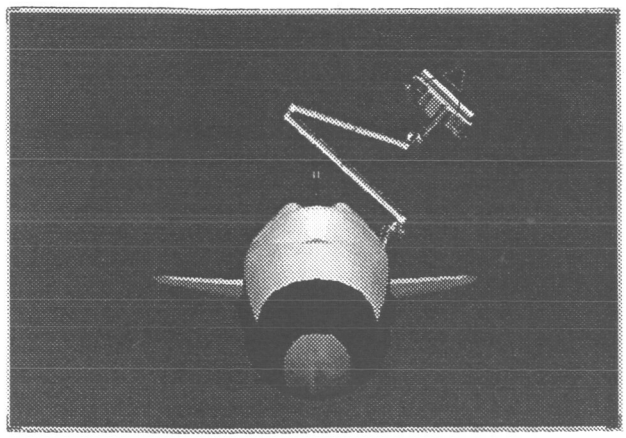

Figure 6 - POR Maneuver Final Configuration

RESULTS

Pertinent kinematic simulation results are presented in Figures 7 through 9. In Figure 7, notice the constant acceleration region (linear velocity profile), the constant maneuver rate region (constant velocity profile), the linear deceleration braking region (parabolic velocity profile), and the active position hold region (zero velocity profile). In Figure 8, the POR Euler attitude time histories represent a great arc rotation that can be more easily seen in the maneuver region of the rotational velocity plot. In Figure 9, the joint responses are smooth and continuous in the separate maneuver regions. In general, the kinematic simulation response is a "perfect" or ideal response.

Figures 10 through 12 represent analogous plots for the dynamic simulation. Notice that upon first glance the position and orientation histories appear almost identical and that the velocity profiles look very similar. This result demonstrates that fundamental controllability of the POR position and orientation is achievable. However, some important differences between the two simulation responses require additional discussion. To help visualize the actual differences between the two simulations, the POR translational vector data from kinematic simulation is subtracted from the dynamic simulation data. The magnitude histories of the resulting "difference", or error, is plotted in Figure 13.

The initial velocity error spike in Figure 13 demonstrates that the instantaneous velocities in the kinematic simulation can not be realistically achieved in a dynamic system. This initial velocity error is the major contributor to the overall POR position error which is close to four inches for this maneuver. However, as shown by the joint angle error histories in Figure 14, the largest arm configuration error occurs during the maneuver region which demonstrates the arm's tendency to drift from the expected configuration.

Returning to Figure 13, small perturbations can be seen during the maneuver region (up to 75 seconds). These perturbations are caused by the most serious control problem we faced while performing these analyses: friction. Compare perturbation time slots in Figure 13 with the time slots in Figure 12 where the joint angle histories change direction, i.e., when the joint velocities become zero. These regions are dominated by joint friction. The velocity perturbations in these regions are caused when 1) the joint initially stops due to friction, and 2) when the joint overcomes friction and breaks loose. Both instances cause discontinuities in the arm motion effectively reducing the system degrees of freedom to something less than seven; this will create problems when the control system expects seven full degrees of freedom to be available for control. Friction problems prompted us to develop the friction compensation logic (only touched upon in this paper) greatly improving our overall arm response (as is evident with the four inch maximum path deviation). We also believe these perturbations can be significantly reduced by placing the low frequency portion of the friction compensation logic with the high frequency portion of the logic.

The second velocity spike of Figure 13 occurs at the beginning of the deceleration region, much like the first spike. The secondary spikes occurring around 90 seconds are caused by a control mode change between the deceleration and active position hold regions. This mode change is primarily a friction compensation gain logic change to allow a finer control for position hold. Notice that the final positional error is less than half an inch.

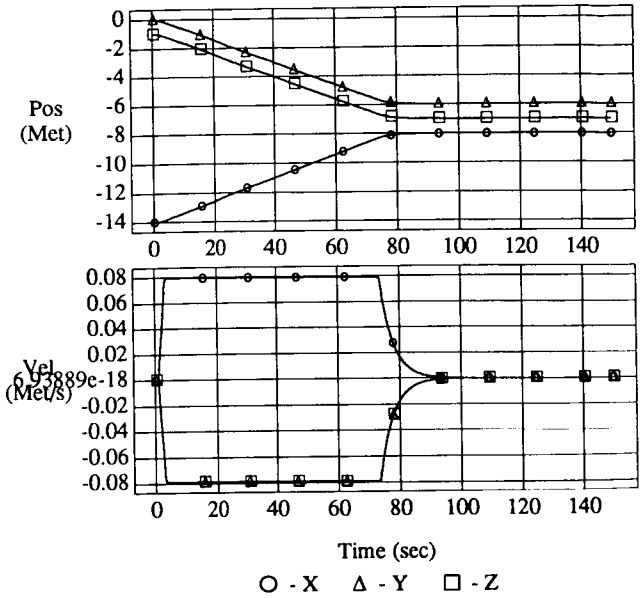

Figure 7 - Kinematic Simulation POR Position and Translational Velocity Histories

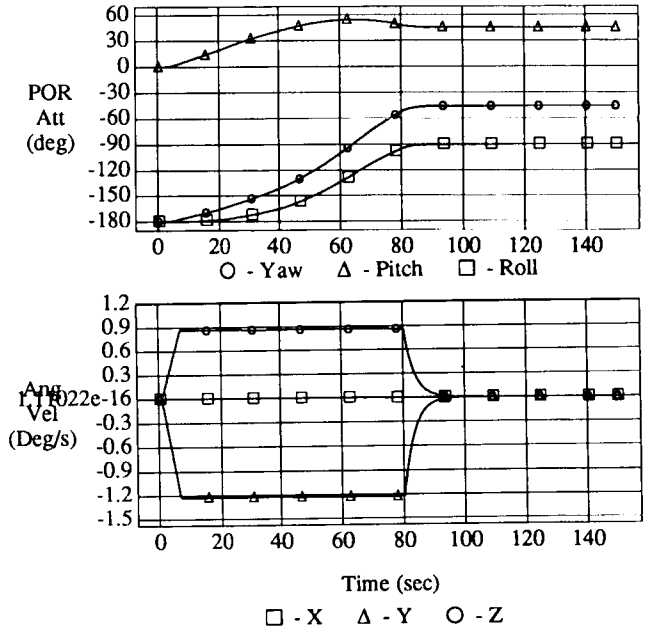

Figure 8 - Kinematic Simulation POR Orientation and Rotational Velocity Histories

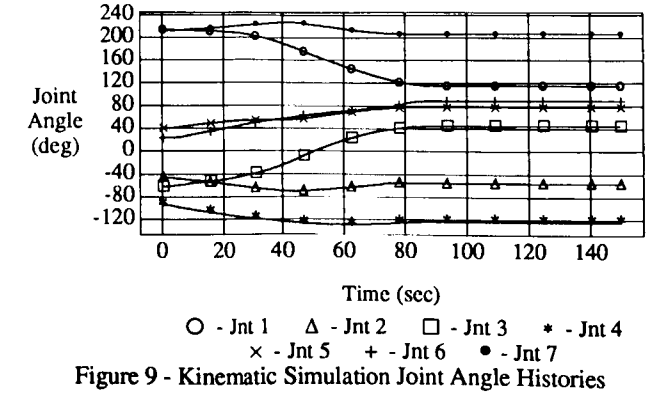

Figure 9 - Kinematic Simulation Joint Angle Histories

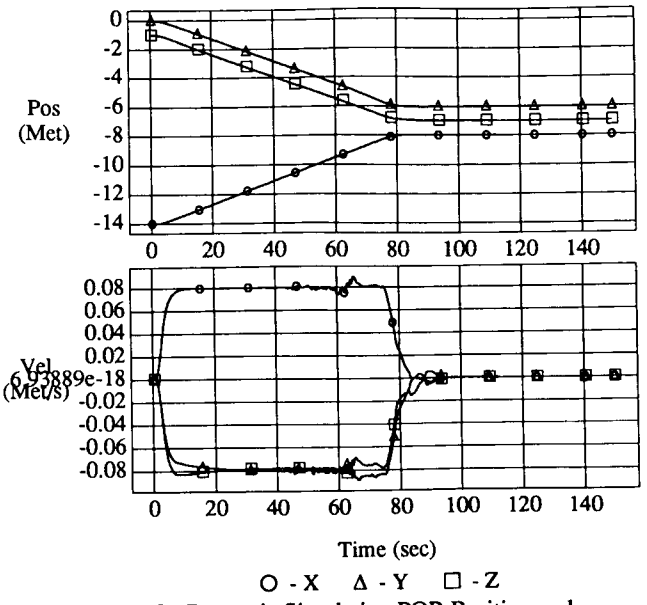

Figure 10 - Dynamic Simulation POR Position and Translational Velocity Histories

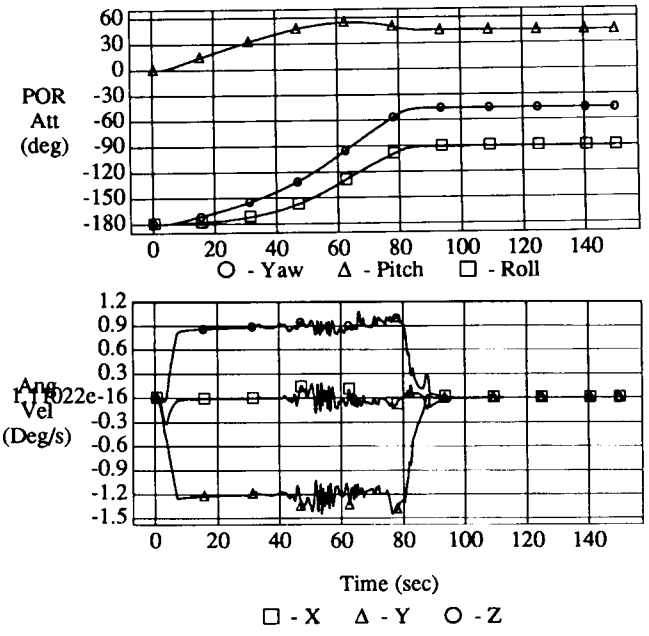

Figure 11 - Dynamic Simulation POR Orientation and Rotational Velocity Histories

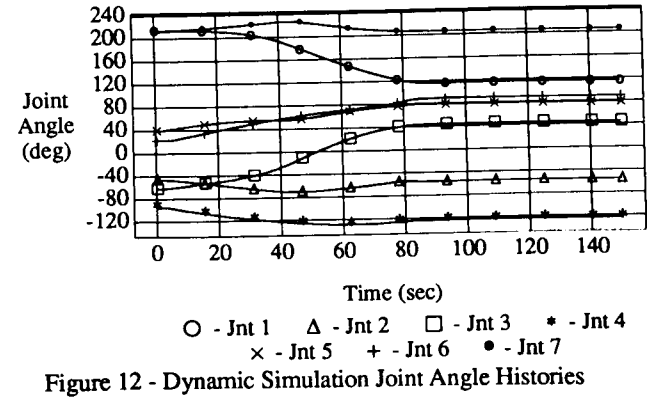

Figure 12 - Dynamic Simulation Joint Angle Histories

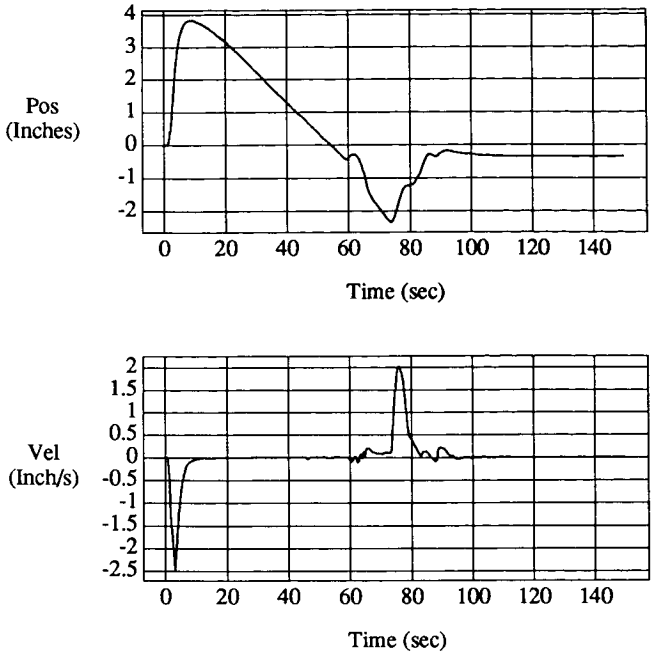

Figure 13 - POR Position and Translational Velocity Difference (Dynamic Simulation - Kinematic Simulation)

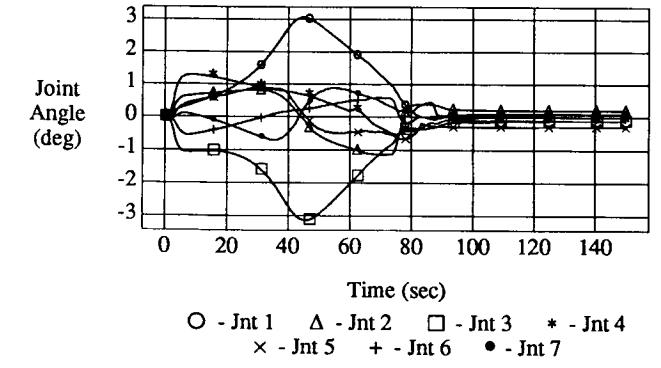

Figure 14 - Joint Angle Difference History

Substituting the POR force and torque control mode during the acceleration and deceleration regions produces interesting results. Figure 15 shows Figure 13 with overplots of the POR force/torque control simulation. Notice how the force/torque control responds much faster to the initial rate command than does the rate control (0 to 5 second region). Also notice the same to be true during the deceleration region (75 to 90 seconds). The most interesting aspect of the force/torque overplot is the large velocity spikes near 80 seconds. These spikes are again caused by joint friction and they are much more pronounced than the friction spikes of the rate control regions. This can be attributed to the difference in rate feedback frequencies; rate feedback for the force/torque control occurs at 12.5 Hz whereas the rate feedback for the rate control occurs at 200 Hz. Obviously, the rate controller will be able to react much better to discontinuities than the force/torque controller. However, even with the large velocity spikes the addition of the POR force/torque control improved the overall path deviation throughout the maneuver.

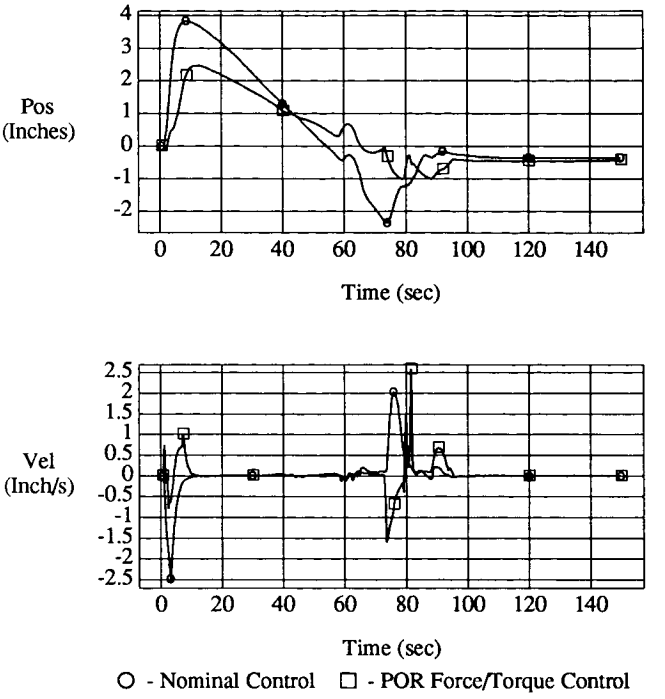

Figure 15 - POR Force/Torque Control Comparison

CONCLUSIONS

POR rate control is successfully achieved for kinematically redundant space manipulators and POR maneuvers are generally repeatable. In task space, there is good agreement between kinematic and dynamic simulations. However, arm configurations through the maneuvers are generally not repeatable between kinematic and dynamic simulations which suggests a drawback to complicated task scenario development using kinematic simulations.

The primary goal of most manipulator task scenario development is to reach the successive POR positions and orientation with a benign (no collisions, no singularities, etc.) arm configuration. If the arm configuration is not precisely predictable with a kinematic simulation then one of two events needs to happen. Either analyses should be performed with a reasonably high fidelity dynamic simulation, or a kinematic controller needs to be developed which controls both manipulator task space and configuration space motions.

Although the force/torque controller improved the POR response, the arm configuration drift problem still exists. We believe this problem will never be completely solved until some type of hybrid POR and arm configuration controller is developed to control the task space and configuration space aspects of the problem concurrently. Perhaps an adaptive controller utilizing varying system dynamic characteristics in conjunction with the POR force and torque control principles presented here, or possibly a 6+1 degree-of-freedom (DOF) controller which controls a single joint independently of the others to "fix" a 6 DOF solution for POR rate control.

We also believe that the POR force and torque control scheme presented here can be enhanced to provide rate control equivalent control during the maneuver region. The advantage of this type of controller is that no mathematical singularities exist. The transformation between POR forces and torques and joint torques is the transpose of the Jacobian matrix, a matrix which does *not have to be inverted* and thus will not exhibit control singularities.

REFERENCES

[1] Press, W., Flannery, B., Teukolsky, S., and Vetterling, W., Numerical Recipes in C: The Art of Scientific Computing, Cambridge University Press, Cambridge, Massachusetts, 1988, pp. 580 - 582 .

[2] Whitney, D., "Resolved Motion Rate Control of Manipulators and Human Prostheses," *IEEE Transactions on Man-Machine Systems*, Vol. MMS-10, No. 2, 1969, pp. 47 - 53.

[3] Bailey, R., Quiocho, L, and Cleghorn, T., "Kinematically Redundant Arm Formulations for Coordinated Multiple Arm Applications," *Proceedings of the Third Annual Workshop on Space Operations Automation and Robotics*, 1989, pp. 447 -454.

[4] "SRMS Master Parameters List", SPAR-R.775 H, February 1983.

[5] "PDRS Database", NASA/JSC Letter VP-88-058, March 1988.

[6] "Space Shuttle Operation Level C Functional Subsystem Software Requirements Document Remote Manipulator System (RMS)", STS 87-0017, November 1987.